agriculture

MDPI

Article

# QTL Mapping of Somatic Regeneration-Related Traits in Maize

**Liqiang Dai *, Yan Zhang, Siping Han and Dongyun Hao**

Institute of Agricultural Biotechnology, Jilin Academy of Agricultural Sciences, Changchun 130033, China; zhangyan4023@cjaas.com (Y.Z.); hansp@cjaas.com (S.H.); dyhao@cjaas.com (D.H.)
* Correspondence: lqdai@cjaas.com

**Abstract:** The somatic regeneration of maize depends on its genotypes, so improving its variety with modern biotechnology is severely restricted. Locating the quantitative trait loci (QTLs) associated with somatic regeneration is important for breeding elite inbred lines that undergo genetic transformations. Here, by crossing the high-regeneration inbred line H99 and non-regeneration inbred line Fr993, an $F_2$ population and its $F_{2:3}$ and $F_{2:4}$ population families were constructed. Immature embryos from the family populations were subjected to tissue culture in two independent seasons to determine their embryogenic callus induction rates (EIRs), green callus rates (GCRs) and plantlet regeneration rates (PRRs). Genetic linkage maps were constructed for the $F_2$ population to locate somatic regeneration QTLs. The results showed that variation in the EIR, GCR and PRR ranged from 0.00–99.33%, and their broad-sense heritabilities were 0.50, 0.52 and 0.53, respectively. The total genetic distance of the linkage maps constructed by the GenoBaits 10 K chip was 2319.50 cM, and twelve QTLs were associated with somatic regeneration traits, accounting for 3.90–14.06% of the phenotypic variation. Expression analysis revealed six candidate genes screened from the QTLs with distinct responses to induction culture in the parental lines, suggesting that they may impact commitment to somatic cell fate. These results provide a basis for the molecular breeding of maize varieties with high-frequency somatic regeneration.

**Keywords:** cell totipotency; embryogenic callus (EC); regenerative capacity; maize; candidate genes

check for updates

**Citation:** Dai, L.; Zhang, Y.; Han, S.; Hao, D. QTL Mapping of Somatic Regeneration-Related Traits in Maize. *Agriculture* **2022**, *12*, 393. https://doi.org/10.3390/agriculture12030393

Academic Editors: Ioannis Tokatlidis and Panagiotis Madesis

Received: 9 February 2022
Accepted: 7 March 2022
Published: 11 March 2022



## 1. Introduction

The fate of maize somatic cells can be reprogrammed under the action of hormones and the cells allowed to develop into an independent complete plant through cell division and differentiation, which is the theoretical basis for establishing an efficient regeneration system. However, because knowledge of the induction mechanism of cell totipotency is insufficient, the lack of inbred lines with an excellent ability to regenerate somatic cells has become a bottleneck in the application of gene editing and other technologies in the genetic improvement of maize. Since Green and Philips [1] first used immature maize embryos to induce callus and obtain regenerated plants in 1975, a large number of studies have found that embryogenic callus (EC) is difficult to induce in most maize genotypes and almost no elite inbred lines can regenerate as a result [2–4]; thus, inbred lines do not serve as a direct recipient for foreign genes. Currently, the genetic transformation of maize can be carried out using only a few lines, and the agronomic traits of these lines are suboptimal. If these materials are transformed for production, they must go through multiple generations of backcrossing, which greatly reduces their use value [5,6]. Therefore, locating the quantitative trait loci (QTLs) that control somatic regeneration and breeding inbred lines with a strong regeneration capacity and excellent comprehensive traits are highly significant for accelerating improvements in biotechnology enabling maize variety breeding. Somatic regeneration in maize is mainly divided into the organogenesis and somatic embryogenesis pathways. In both pathways, explant differentiation must be induced to obtain meristematic potential, and then a meristem or embryonic development-like process occurs to form a complete plant. Regeneration capacity varies greatly among

different maize varieties, and this difference is mainly controlled by related genes [7–9]. In addition, the growth state of donor plants and the culture conditions of explants also have a certain impact on regenerated plant formation [10,11].

Previous studies have reported that somatic regeneration in maize is a quantitative trait with predominantly additive effects [12,13]. Krakowsky et al. [14] performed tissue cultures with immature embryos from 127 recombinant inbred lines (RILs) and found that the broad-sense heritability of the embryogenic callus induction rate (EIR) was 0.52, indicating that this trait was greatly influenced by genetic factors. Pan et al. [15] analyzed an $F_2$ population derived from a cross between 18–599 and R15 and found that the broad- and narrow-sense heritabilities of maize EC induction were 0.64 and 0.63, respectively. These results revealed that the heritability of this trait was high and that this trait is suitable for selection in early generations of breeding. Zhang et al. [16] conducted experiments on inbred lines from North America and China. The results showed that the broad-sense heritability of the somatic redifferentiation rate reached 0.75, and the number of plantlets regenerated from EC was as high as 0.74, which confirmed that the somatic regeneration of maize is mainly controlled by genetic factors and that it is feasible to further locate the major genes controlling this trait by molecular methods.

As early as 1992, Armstrong et al. [17] first used restriction fragment length polymorphism (RFLP) markers to analyze the progenies derived from a cross between A188 and Mo17, and the results showed that five loci were closely related to EC induction in maize. Lowe et al. [18] utilized a $BC_1$ population generated by crossing Hi-II and FBLL to identify five chromosomal regions that may control the tissue culture and genetic transformation traits of maize using RFLP and simple sequence repeat (SSR) markers. Ma et al. [19] used 144 inbred lines as an association population and detected a total of 63 single nucleotide polymorphisms (SNPs) that were stably associated with EC regeneration using the maizeSNP50 chip. Forty candidate genes were mined based on these markers, and some genes were linked to auxin transport, cell fate, seed germination and embryonic development. Zhang et al. [20] conducted transcriptome analysis on calli at the early stage of redifferentiation and screened 707 differentially expressed genes that might be involved in the regeneration pathway of maize somatic cells. Ge et al. [21] compared the genome of line A188 with those of three references, including B73, and found that a 3053 kb region on chromosome 3 contains eight large structural variants and two differentially expressed genes that could be related to EC induction in maize. However, due to the limitations of the research materials and the low number of markers used, most of the reported QTLs or candidate genes have only a minor effect on somatic regeneration; it is still not possible to determine the major factors controlling this trait.

In this study, we chose the high-regeneration line H99 which is widely applied in maize genetic transformation instead of the ordinary lines used in previous studies. An $F_2$ population and corresponding $F_{2:3}$ and $F_{2:4}$ population families were constructed by crossing H99 with the non-regeneration line Fr993. Subsequently, genetic linkage maps of the $F_2$ population were constructed for the first time using a high-density gene chip containing 67 K SNPs. The linkage analysis results revealed that a total of twelve QTLs were associated with EIR and plantlet regeneration rate (PRR). Among these loci, six candidate genes, *Zm00001d043076* (*WOX13a*), *Zm00001d047879* (*CLE16*), *Zm00001d002495* (*AHL23*), *Zm00001d043431* (*ARF11*), *Zm00001d043205* (*EREB147*) and *Zm00001d028930* (*MYB75*), were preliminarily verified which may be involved in determining the fate of maize cells. The findings of this study lay a foundation for molecular marker-assisted selection of inbred lines that can undergo somatic regeneration with a high frequency and for the further analysis of totipotency induction mechanisms in plant cells.

## 2. Materials and Methods

### *2.1. Plant Materials and Field Design*

The inbred line H99 (Illinois Synthetic 60 C) [22], which has a strong somatic regeneration capacity and is widely used in the genetic transformation of maize, was used as

the female parent, and the line Fr993 (Reid germplasm), which could not be regenerated due to induced nonembryogenic callus (NEC), was used as the male parent. In the summer of 2019, hybridization was carried out at the experimental field of the Jilin Academy of Agricultural Sciences (43°30′ N, 124°48′ E) in Gongzhuling, China. In December of the same year, five $F_1$ plants were self-pollinated in the Ledong experimental field (18°44′ N, 108°98′ E) in Hainan, China. In February 2020, the $F_2$ population was planted in Ledong, and 213 plants were randomly selected for self-pollination to generate corresponding $F_{2:3}$ population families. In May 2020, the parental lines and $F_{2:3}$ population families were planted in Gongzhuling. Each line was planted in a single row that was 4 m long, the row spacing was 0.6 m, and there were 16 plants per line with three replications. When the maize reached the flowering period, the plants from each family were self-pollinated, and the harvested seeds were of the $F_{2:4}$ family. In May 2021, the parents and $F_{2:4}$ population families were grown in Gongzhuling, and the field experimental design and management were identical to those in 2020. For the above populations, the genomic DNA of 213 $F_2$ plants was utilized to construct genetic linkage maps, and the $F_{2:3}$ and $F_{2:4}$ population families were used to quantify somatic regeneration-related traits.

### *2.2. Trait Evaluation*

In 2020 and 2021, self-pollination was performed when the parental lines and segregating populations reached the flowering period. Approximately 9 to 12 d after pollination, two ears were picked from each plot, and 25 immature embryos with a length of approximately 1.5 mm were stripped from each ear and transferred to the induction medium. The embryos were cultured in the dark at 28 °C for 4 weeks with the convexity up and the plane down. During this period, the explants were subcultured once, and the adventitious shoots and roots were removed in a timely manner. After induction culture, the number of ECs induced from each ear was counted, and EIRs were calculated according to the following formula:

$$\text{EIR (\%)} = (\text{number of ECs/number of immature embryos}) \times 100\%. \quad (1)$$

Subsequently, the ECs were transferred to differentiation medium with the unit of embryos and cultured at 25 °C for 16 h under 2000 lx light every day. When the ECs had differentiated for 2 weeks, the explants were subcultured once, the number of ECs with green spots on the surface was counted, and green callus rates (GCRs) were calculated according to the formula:

$$\text{GCR (\%)} = (\text{number of ECs with green spots/number of immature embryos}) \times 100\%. \quad (2)$$

When the cultures had differentiated for 4 weeks, the number of ECs with regenerated plantlets longer than 1 cm was counted, and PRRs were calculated as follows:

$$\text{PRR (\%)} = (\text{number of ECs with regenerated plantlets longer than 1 cm/number of immature embryos}) \times 100\%. \quad (3)$$

The average values of the EIR, GCR, and PRR among three replications for each family in 2020 and 2021 and the general average of the two-year data for each $F_2$ plant were used for further analysis. The phenotypic characteristics of the cultures are shown in Figure 1, and medium composition details are provided in Tables S1 and S2.

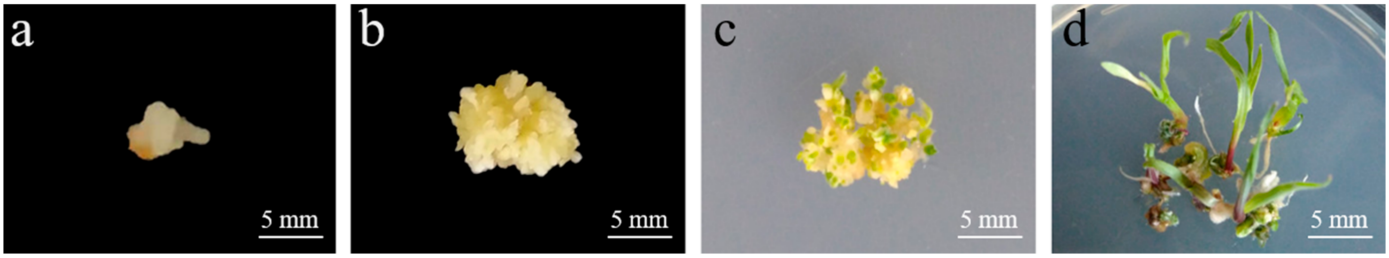


**Figure 1.** Features of the cultures during induction and differentiation stages. (**a**) Non-embryogenic callus (NEC). (**b**) Embryogenic callus (EC). (**c**) EC with green spots. (**d**) Regenerated plantlets. Bars = 5 mm.

### *2.3. Phenotypic Statistical Analysis*

Descriptive statistical analysis, correlation analysis, and normality tests were performed on the phenotypic data using SPSS 24.0 (IBM Corp., Armonk, NY, USA). The *p*-values for standard deviations (SDs) were calculated by two-tailed Student's *t*-test. Data from three replicates in each year were subjected to variance analysis using the "anova" command in R 4.0.0 (https://www.r-project.org/, accessed on 5 January 2022) to assess the significance of genotype, environment and their interactional effects. The broad-sense heritability of the EIR, GCR and PRR was calculated according to the formula proposed by Knapp et al. [23] as follows:

$$H^2 = \delta G^2/[\delta G^2 + (\delta GE^2/\mathrm{e}) + \delta \mathrm{r}^2/\mathrm{re}] \quad (4)$$

where $\delta G^2$ is the genetic variance, $\delta GE^2$ is the genotype-by-environment interaction variance, $\delta \mathrm{r}^2$ is the residual error, e is the number of environments and r is the number of replications.

### *2.4. Genotyping, Construction of Linkage Maps and QTL Detection*

Leaf genomic DNA was extracted from the parental inbred lines, $F_1$ plants and $F_2$ individuals using a Hi-DNAsecure Plant Kit (Tiangen, Beijing, China). To assess DNA quality, 1% agarose gel electrophoresis was performed, and a Qubit 2.0 system was utilized (Invitrogen, Waltham, MA, USA). Qualified samples were genotyped using the GenoBaits 10 K chip [24], which was developed based on the genotyping by target sequencing (GBTS) platform. According to the genotyping results, polymorphic SNPs between the two parents were screened, and partially segregating and duplicate markers were removed using JoinMap 4.0 [25]. Genetic linkage maps of the $F_2$ population were constructed using MAPMAKER 3.0 [26], and the linkage groups were identified using the "Group" command with a logarithm of odds (LOD) threshold of 3.0. Finally, the recombination frequencies were converted to centiMorgan (cM) using the Kosambi mapping function [27].

QTL detection was performed using the composite interval mapping (CIM) method [28] in WinQTL Cartographer 2.5 [29] combined with the phenotypic data of the somatic regeneration traits and genetic linkage maps. Significance thresholds for screening putative QTLs were obtained by performing 1000 permutations at $p < 0.05$ for each dataset.

### *2.5. Candidate Gene Predictions and Expression Analysis*

Based on the flanking markers of the detected QTLs, the reference genome RefGen_v4 (ftp.gramene.org/pub/gramene/release-63/fasta/zea_mays/dna/, accessed on 20 January 2022) of B73 was used to screen for candidate genes that may control somatic regeneration. Annotated functions and relevant information for the genes were obtained from the MaizeGDB database (https://www.maizegdb.org/, accessed on 24 January 2022) and MaizeSequence (http://ensembl.gramene.org/Zea_mays/Info/Index/, accessed on 24 January 2022). Six candidate genes, *WOX13a*, *CLE16*, *AHL23*, *ARF11*, *EREB147* and *MYB75*, were randomly selected to examine differences in expression patterns during the callus

induction period of the parental lines H99 and Fr993. First, total RNA was extracted from the cultures at five callus induction stages (0 d, 4 d, 8 d, 12 d and 16 d) using a Plant Total RNA Isolation Kit (Sangon, Shanghai, China). Subsequently, RNA was reverse-transcribed into cDNA using MightyScript Plus First Strand cDNA Synthesis Master Mix (gDNA digester) (Sangon, Shanghai, China). qPCR detection was performed with a StepOnePlus Real-Time PCR System (Applied Biosystems, USA) using TB Green Premix Taq (TaKaRa, Beijing, China). The amplification reaction conditions included predenaturation at 95 °C for 30 s and 40 cycles of 95 °C for 5 s and 60 °C for 30 s. The gene *Zm00001d049641* (*GADPH*) was used as the internal control, and all reactions were performed three times. Finally, the fold-changes of the six target genes were calculated using the $2^{-\Delta\Delta CT}$ method [30]. The primers used in qPCR were designed with Primer Premier 5.0 (PREMIER Biosoft International, Palo Alto, CA, USA), and the detailed sequence information is provided in Table S3.

## 3. Results

### 3.1. Phenotypic Variation

To identify the capacity of the maize $F_2$ population to undergo somatic regeneration, immature embryos from two parental lines and the $F_{2:3}$ and $F_{2:4}$ population families derived from 213 $F_2$ individuals were used to perform tissue cultures, and their EIRs, GCRs and PRRs were calculated. In 2020 and 2021, the average EIR, GCR and PRR of the parent (H99) that possessed a strong regeneration capacity reached 83.29%, 82.64% and 80.25%, respectively, while the values in the non-regeneration parent Fr993 were all 0. In the segregating populations, the EIR, GCR and PRR varied from 0.00–99.33%, with averages of 41.59%, 40.20% and 37.70%, respectively (Tables 1 and S4). The SDs of the three traits ranged from 17.64% to 23.69% (Table 1), showing high values and revealing that genetic factors may have had a strong influence on phenotypic variation. In addition, the *p*-values for the SDs were all less than 0.01, indicating significant variation in somatic regeneration capacity in this population (Table 1). Kolmogorov–Smirnov tests showed that the averages of the two-year phenotypes for 213 $F_2$ plants were all normally distributed (Figure 2), and their phenotypes in 2020 and 2021 also showed only a slight left skew (Figure S1). Thus, somatic regeneration in maize is a quantitative trait controlled by multiple genes. Further Pearson's correlation analysis was performed on the EIR, GCR and PRR, and the correlation coefficients between them ranged from 0.978 to 0.992 (Figure 2), indicating that somatic dedifferentiation induced totipotency, and the response of EC to light culture at the early stage of differentiation was closely associated with the formation of regenerated plantlets.

**Table 1.** Phenotypic performance of somatic regeneration traits in the maize segregating populations.

| Environment | EIR (%) | | GCR (%) | | PRR (%) | |
|---|---|---|---|---|---|---|
| | Range | Mean ± SD [1] | Range | Mean ± SD | Range | Mean ± SD |
| 2020 | 0.00–90.49 | 33.32 ± 20.93 ** | 0.00–83.51 | 32.18 ± 20.76 ** | 0.00–81.36 | 29.07 ± 19.60 ** |
| 2021 | 4.67–99.33 | 49.86 ± 22.22 ** | 2.00–99.33 | 48.21 ± 22.92 ** | 1.33–99.33 | 46.33 ± 23.69 ** |
| Average | 5.77–87.06 | 41.59 ± 17.64 ** | 3.10–87.06 | 40.20 ± 17.95 ** | 1.58–85.81 | 37.70 ± 17.89 ** |

[1] SD: standard deviation; **: $p \leq 0.01$.

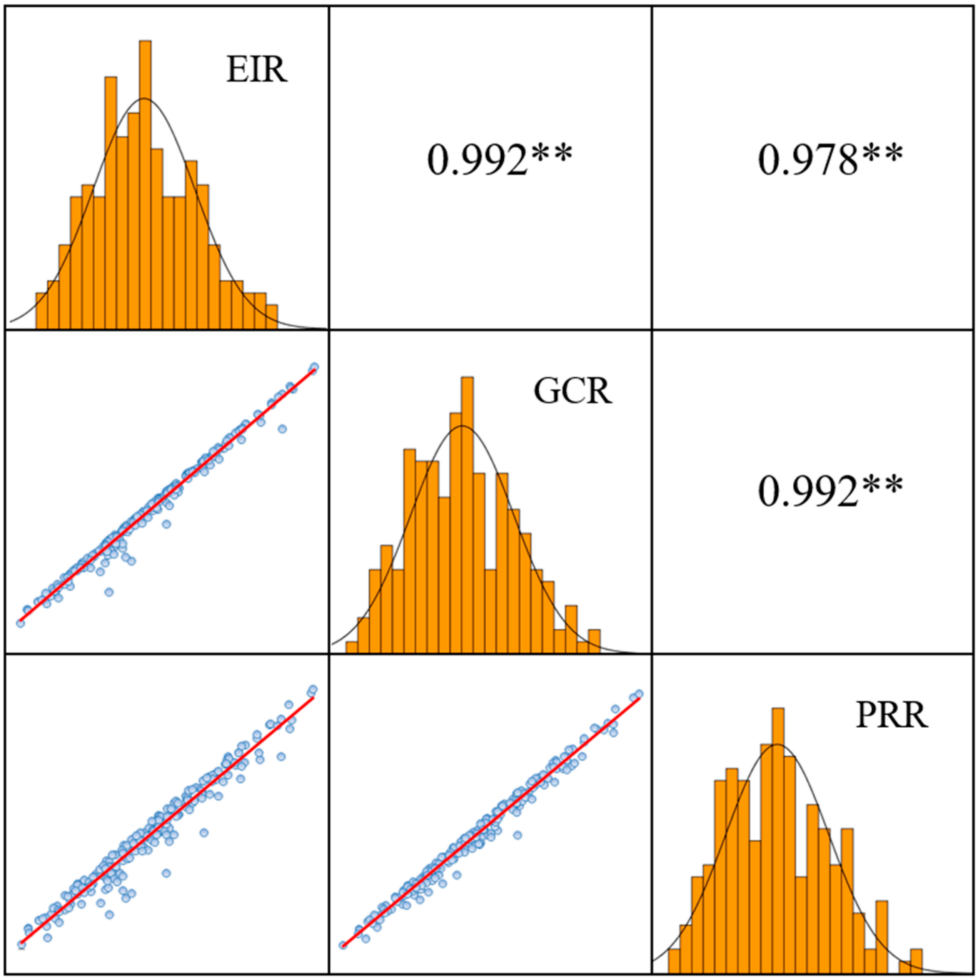


**Figure 2.** Distributions and correlations between three somatic regeneration traits with the average value across two years. The plots on the diagonal line show the phenotypic distributions of the EIR, GCR and PRR. The values above the diagonal line are Pearson's correlation coefficients between every pair of traits. The scatter plots of correlations are shown in the areas below the diagonal, and the red lines in the plots represent the correlation trends. **: $p \leq 0.01$; EIR: embryogenic callus induction rate; GCR: green callus rate; PRR: plantlet regeneration rate.

### *3.2. Heritability of Somatic Regeneration Traits*

The broad-sense heritabilities of the EIR, GCR and PRR were calculated using the formula proposed by Knapp et al. [23] based on analysis of variance of the three traits. The variance analysis revealed significant effects ($p < 0.01$) of genotype, the environment, and their interaction on the EIR, GCR and PRR (Table 2), and there was no significant variation among replicates for any of the traits, indicating that somatic regeneration in maize is controlled by genotype and its interaction with the environment. The broad-sense heritability values for the EIR, GCR and PRR were all moderate, equaling 0.50, 0.52 and 0.53, respectively. This confirmed that the phenotypic variation in somatic regeneration in this population was mainly derived from genetic factors, indicating suitability for further QTL mapping. Finally, after considering the heritability and correlation analysis results for the three traits, we removed the GCR, which was highly correlated with the PRR (r = 0.992) during redifferentiation. Therefore, the following linkage analysis was performed only with the EIR and PRR at two different culture stages.

**Table 2.** Analysis of variance for the EIR, GCR and PRR.

| Trait | Source [1] | *Df* [2] | *SS* [3] | *MS* [4] | *F*-Value | *Pr* (>*F*) [5] | Significance [6] |
|---|---|---|---|---|---|---|---|
| EIR | *G* | 212 | 36.82 | 0.17 | 9.53 | $<2.0 \times 10^{-16}$ | *** |
| | *E* | 1 | 8.37 | 8.37 | 459.13 | $<2.0 \times 10^{-16}$ | *** |
| | *R* | 2 | 0.06 | 0.03 | 1.58 | 0.21 | |
| | $G \times E$ | 212 | 18.27 | 0.09 | 4.72 | $<2.0 \times 10^{-16}$ | *** |
| | Residuals | 772 | 14.08 | 0.02 | | | |
| GCR | *G* | 212 | 38.12 | 0.18 | 9.78 | $<2.0 \times 10^{-16}$ | *** |
| | *E* | 1 | 7.86 | 7.86 | 427.51 | $<2.0 \times 10^{-16}$ | *** |
| | *R* | 2 | 0.05 | 0.03 | 1.45 | 0.24 | |
| | $G \times E$ | 212 | 18.47 | 0.09 | 4.74 | $<2.0 \times 10^{-16}$ | *** |
| | Residuals | 772 | 14.19 | 0.02 | | | |
| PRR | *G* | 212 | 37.72 | 0.18 | 10.15 | $<2.0 \times 10^{-16}$ | *** |
| | *E* | 1 | 9.15 | 9.15 | 521.71 | $<2.0 \times 10^{-16}$ | *** |
| | *R* | 2 | 0.05 | 0.03 | 1.55 | 0.21 | |
| | $G \times E$ | 212 | 17.91 | 0.08 | 4.82 | $<2.0 \times 10^{-16}$ | *** |
| | Residuals | 772 | 13.54 | 0.02 | | | |

[1] *G*: genotype; *E*: environment; *R*: replication; $G \times E$: interaction of genotype and the environment. [2] *Df*: degrees of freedom. [3] *SS*: sum of squares. [4] *MS*: mean squares. [5] *Pr*: probability. [6] ***: significance at $p < 0.001$.

### 3.3. Genotyping and Linkage Map Construction

To construct the genetic linkage maps of the segregating populations, we used the GenoBaits 10 K chip to genotype the genomic DNA of the parental inbred lines, $F_1$ plants and 213 $F_2$ individuals. A total of 67,303 loci were genotyped on the ten chromosomes of maize. Among them, chromosome 1 has the most loci (9738) and chromosome 10 has the least (4796). Based on the genotype data from $F_1$ plants, approximately 37.47% of the SNP loci were heterozygous, and their alleles had very high (99.84%) fidelity to the two parental lines. This result indicates that hybridization was successful and that the genotyping quality was good. Subsequently, the loci with polymorphisms between the parents H99 and Fr993 were screened, and partially segregating and repetitive markers were further removed. Finally, the remaining 1283 SNPs were used to construct population genetic linkage maps. A total of 512 SNPs were evenly mapped to ten linkage groups in maize using MAPMAKER 3.0. The total genetic distance of the maps was 2319.50 cM, and the average genetic distance between adjacent SNPs was only 4.53 cM (Table S5), which satisfied the requirements for subsequent QTL detection.

### 3.4. QTL Mapping

Combined with the genetic linkage maps that were constructed and two years of phenotypic data, the CIM method was used to locate the QTLs that control the EIR and PRR. A total of twelve somatic regeneration QTLs were detected on chromosomes 1, 2, 3, 6 and 9, which accounted for 3.90–14.06% of the phenotypic variance (Table 3). Four of the QTLs that controlled the EIR (*qEIR1.1*, *qEIR2.1*, *qEIR3.1* and *qEIR9.1*) were derived from the regenerative parent H99, and these QTLs accounted for 40.49–44.22% of the total phenotypic variation (Figure 3 and Table 3). The regeneration alleles *qEIR1.1* and *qEIR9.1* were detected in two environments and resulted in the highest LOD values of 6.60 and 7.15, respectively, indicating that these two loci were closely related to EC induction in maize. In addition, the modes of gene action for *qEIR1.1*, *qEIR2.1* and *qEIR3.1* were dominated by additive effects, while the gene action of *qEIR9.1* was both additive and dominant (Table 3). Eight QTLs (*qPRR1.1*, *qPRR1.2*, *qPRR2.1*, *qPRR3.1*, *qPRR3.2*, *qPRR6.1*, *qPRR9.1* and *qPRR9.2*) were linked to the PRR, and they were derived from the parental line H99, which explained 69.44–71.36% of the total phenotypic variance (Figure 4 and Table 3). The allele *qPRR2.1* was detected in two environments, and the highest LOD value was 5.82, indicating that this locus was closely related to somatic regeneration in maize. Finally, the QTLs *qPRR1.2*, *qPRR2.1*, *qPRR3.2*, *qPRR9.1* and *qPRR9.2* exhibited predominantly additive

effects, while the gene action of *qPRR1.1*, *qPRR3.1* and *qPRR6.1* was predominantly additive and dominant (Table 3).

**Table 3.** Information on the quantitative trait loci (QTLs) identified for the EIR and PRR.

| QTL | Chr. [1] | Environment [2] | Flanking Markers | Support Interval (cM) | LOD | SRA [3] | $R^2$ (%) [4] | Genetic Effect | | | Mode of Gene Action [5] |
|---|---|---|---|---|---|---|---|---|---|---|---|
| | | | | | | | | Additive | Dominant | Dominance Degree (*d*/*a*) | |
| *qEIR1.1* | 1 | 2021 | p1463773–p1123859 | 85.00–114.60 | 5.65 | H99 | 13.47 | 0.12 | −0.01 | −0.11 | A |
| | | AVE | p1463773–p1123859 | 85.00–114.60 | 6.60 | H99 | 11.62 | 0.09 | 0.01 | 0.07 | A |
| *qEIR2.1* | 2 | AVE | p2652100–p2181844 | 24.40–53.30 | 5.18 | H99 | 8.96 | 0.07 | 0.00 | −0.02 | A |
| *qEIR3.1* | 3 | 2020 | p3187420–p3207764 | 138.10–165.80 | 6.02 | H99 | 11.21 | 0.10 | −0.01 | −0.05 | A |
| *qEIR9.1* | 9 | 2020 | p9110946–p9150912 | 105.20–152.20 | 7.15 | H99 | 8.70 | 0.08 | 0.01 | 0.17 | A |
| | | AVE | p9110946–p9150912 | 105.20–152.20 | 6.55 | H99 | 10.58 | 0.08 | −0.02 | −0.22 | PD |
| *qPRR1.1* | 1 | 2021 | p1308356–p1463773 | 61.00–85.00 | 5.00 | H99 | 4.78 | 0.07 | 0.05 | 0.73 | PD |
| *qPRR1.2* | 1 | AVE | p1463773–p1123859 | 85.00–114.60 | 6.46 | H99 | 10.95 | 0.09 | 0.01 | 0.09 | A |
| *qPRR2.1* | 2 | 2021 | p2652100–p2181844 | 24.40–53.30 | 4.11 | H99 | 9.23 | 0.10 | −0.02 | −0.18 | A |
| | | AVE | p2652100–p2181844 | 24.40–53.30 | 5.82 | H99 | 11.15 | 0.08 | −0.01 | −0.17 | A |
| *qPRR3.1* | 3 | 2020 | p3190353–p3207764 | 140.90–165.80 | 6.02 | H99 | 14.06 | 0.11 | −0.04 | −0.33 | PD |
| *qPRR3.2* | 3 | AVE | p3177855–p3193521 | 124.70–151.40 | 4.08 | H99 | 8.03 | 0.07 | −0.01 | −0.18 | A |
| *qPRR6.1* | 6 | AVE | p6162268–p6165840 | 136.50–151.70 | 4.02 | H99 | 3.90 | 0.05 | 0.01 | 0.28 | PD |
| *qPRR9.1* | 9 | 2020 | p9110946–p9150912 | 105.20–152.20 | 7.35 | H99 | 9.37 | 0.08 | 0.01 | 0.14 | A |
| *qPRR9.2* | 9 | AVE | p9207083–p9112764 | 70.80–94.50 | 5.98 | H99 | 9.12 | 0.07 | −0.01 | −0.19 | A |

[1] Chr.: chromosome. [2] AVE: average of the two-year data for each $F_2$ plant. [3] SRA: source of the regeneration allele. [4] $R^2$: percentage of the phenotypic variation explained by the QTL. [5] A: additive, an absolute value of the dominance degree between 0.00 and 0.20; PD: partially dominant, an absolute value of the dominance degree between 0.20 and 0.80.

By comparing the QTL intervals of the two traits, we found that all four QTLs for the EIR were located within the loci obtained for the PRR (Figure 5 and Table 3). Among them, the QTLs *qEIR1.1*, *qEIR2.1* and *qEIR9.1* were completely consistent with *qPRR1.2*, *qPRR2.1* and *qPRR9.1* in terms of their support intervals, respectively, while the *qEIR3.1* support interval partially overlapped with those of *qPRR3.1* and *qPRR3.2*, respectively. After all somatic regeneration QTLs were further integrated, a total of five segments were distributed on chromosomes 1, 2, 3, 6 and 9, and their combined length was approximately 12.74% of the entire maize genome length (Figure 5). Within the above physical ranges, we screened 5 WUSCHEL (*WUS*) family genes (*WOX2a*, *WOX5b*, *WOX6*, *WOX11* and *WOX13a*), including the embryonic transcription factor *WOX2a*, 4 stem cell characteristic CLAVATA3/ESR (*CLE*) family genes (*CLE2*, *CLE6*, *CLE16* and *CLE22*), 4 auxin signal transduction pathway genes (*IAA12*, *IAA30*, *ARF11* and *ARF23*), 6 AT-hook motif nuclear-localized protein (*AHL*) family genes (*AHL1*, *AHL13*, *AHL22*, *AHL23*, *AHL25* and *AHL27*) and 30 *MYB* family transcription factors. The resulting genes can serve as potential candidate genes for controlling somatic regeneration in maize.

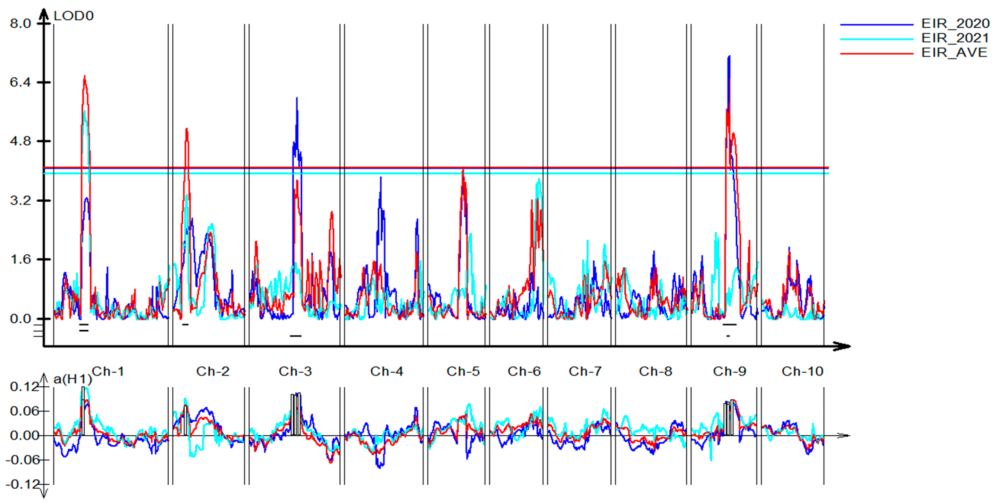


**Figure 3.** Detection of quantitative trait loci (QTLs) for the EIR in the segregating population. The log of odds (LOD) and additive effect, a(H1), plotted against the ten chromosomes were used for linkage analysis. The horizontal lines represent the threshold values for detecting authentic QTLs.

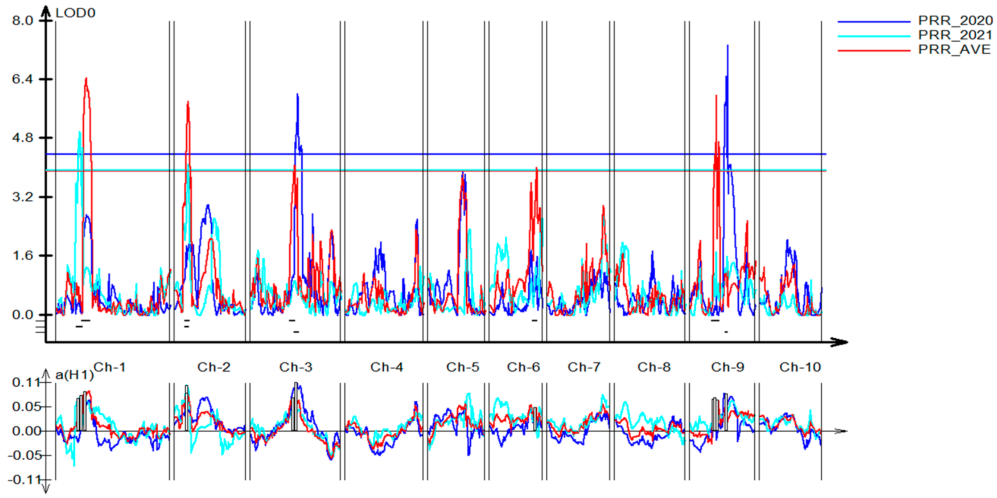


**Figure 4.** Detection of quantitative trait loci (QTLs) for the PRR in the segregating population. The log of odds (LOD) and additive effect, a(H1), plotted against the ten chromosomes were used for linkage analysis. The horizontal lines represent the threshold values for detecting authentic QTLs.

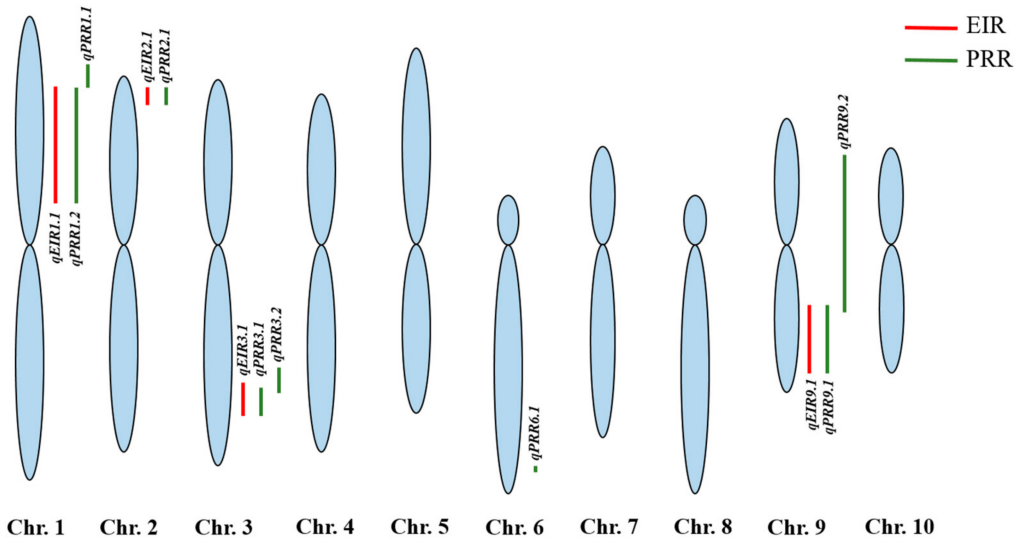


**Figure 5.** Distribution of somatic regeneration quantitative trait loci (QTLs) on maize chromosomes. The red and green bars represent QTL intervals of the EIR and PRR, respectively. Chr.: chromosome.

### *3.5. Expression Analysis of the Candidate Genes*

To preliminarily verify the function of the candidate genes in somatic regeneration, we randomly selected six genes and quantified their levels of expression at different stages (0 d, 4 d, 8 d, 12 d and 16 d) of callus induction in the segregating population parents H99 (PRR = 80.25%) and Fr993 (PRR = 0). The results indicated that the fold-changes of the *WOX13a* gene in H99 gradually increased with prolonged induction time, and its expression was maximal when the explants were cultured for 8 d, after which it decreased (Figure 6a). However, the expression of this gene in Fr993 remained almost stable in each stage of induction culture. The expression of the *CLE16* gene in the two inbred lines showed a trend of first increasing and then decreasing. It peaked when H99 was induced for 8 d and Fr993 was induced for 4 d (Figure 6b). Meanwhile, the fold-changes of *CLE16* in Fr993 were generally higher than those in H99. The expression of the *AHL23* gene gradually increased with culture time, and its expression in each induction stage was higher in H99 than in Fr993 (Figure 6c). In addition, the expression of the *ARF11* gene in H99 first decreased and then returned to its initial level (Figure 6d). However, the expression of this gene in Fr993 decreased rapidly from the beginning of induction and finally reached a lower level. Finally,

the fold-changes of *EREB147* and *MYB75* in the two parental lines also exhibited distinct differences, respectively (Figure 6e,f). The above results confirmed that the expression patterns of the candidate genes differed between maize lines with different regeneration capacities. The divergent responses of these genes to induction culture may be essential for somatic cells to successfully acquire totipotency.

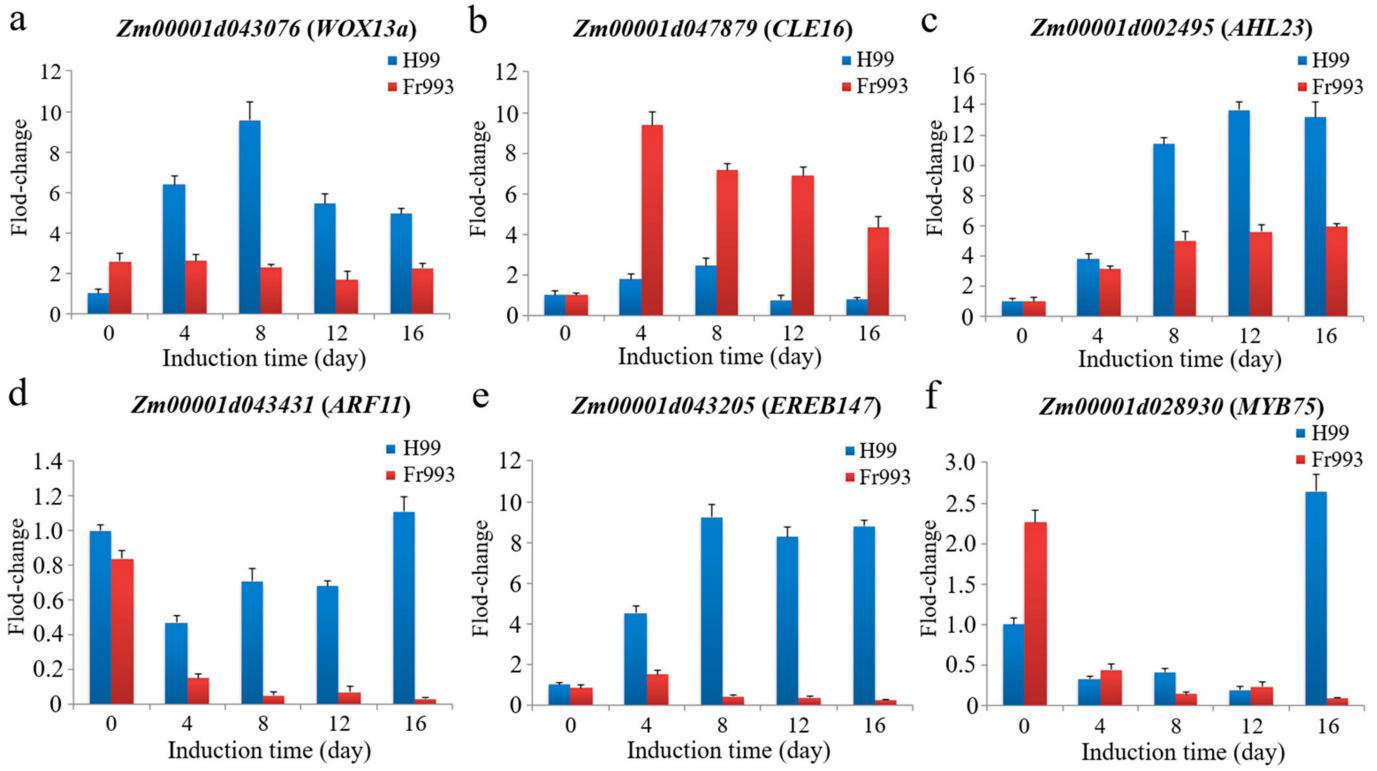


**Figure 6.** Expression profiles of the candidate genes at different induction stages. Here, H99 is a line with a high PRR (80.25%) and Fr993 is unable to regenerate. (**a**–**f**) Fold-changes of *Zm00001d043076* (*WOX13a*), *Zm00001d047879* (*CLE16*), *Zm00001d002495* (*AHL23*), *Zm00001d043431* (*ARF11*), *Zm00001d043205* (*EREB147*) and *Zm00001d028930* (*MYB75*).

## 4. Discussion

Plant EC induction is often regarded as the initial step of somatic regeneration [31–34]. However, reports in recent years have shown that not all maize varieties have high EC-based regeneration capacities, and some lines cannot be regenerated at all [35,36], indicating that the embryogenic acquisition and redifferentiation of somatic cells may be controlled by different functional genes. Zhang et al. [16] studied the EC redifferentiation traits of 144 inbred lines and found that the average callus differentiation rate among different materials in three environments was only 15.74–19.52%, while the browning rate was as high as 34.27–42.14%. This indicated that although maize inbred lines can induce embryogenic tissue, their differentiation capacity is generally poor, so they cannot be used as direct recipients of foreign genes. In this study, we crossed the inbred line H99, which is widely used in maize genetic transformation, and the non-regeneration line Fr993. By phenotyping two offspring family populations, we revealed that the phenotypic correlation coefficients between the EIR, GCR and PRR were all above 0.97 (Figure 2), indicating that as long as these segregating populations can induce ECs, regenerated plantlets can almost be obtained after differentiation culture. These results are completely different from those of studies that used inbred line populations as research materials, indicating that there may be multiple superior alleles that are closely linked or major genes that control both EC induction and plantlet regeneration in the parent H99, and this is an ideal genotype for researching the somatic regeneration of maize. The broad-sense heritabilities of the EIR,

GCR and PRR were further calculated to be 0.50, 0.52 and 0.53, respectively. These values were in the range of 0.48–0.79 obtained in previous studies [14–16], which is indicative of a moderate heritability level; therefore, it is feasible to locate the QTLs that control somatic regeneration in maize.

A total of twelve QTLs closely associated with the EIR and PRR were mapped in this study (Figure 5 and Table 3). Among them, the support intervals of four EIR QTLs (*qEIR1.1*, *qEIR2.1*, *qEIR3.1* and *qEIR9.1*) were all located within the loci obtained for the PRR (Figure 5 and Table 3), which was related to the high regeneration capacity exhibited by EC from the segregating population. In addition, three unique QTLs (*qPRR1.1*, *qPRR6.1* and *qPRR9.2*) were also detected for the PRR (Figure 5), suggesting the presence of specific genes within these genomes that control the redifferentiation of EC. By further comparing the above sites with those reported in previous studies, we found that *qPRR3.2* contains a 3053 kb region that controls the embryogenic tissue culture response and plant regeneration of maize [37]. Eight genes with large structural variants and two differentially expressed genes were mined in this area, which may be responsible for the induction of EC in maize [21]. Ma et al. [19] found a significant marker, PZE-103123331, that was stably associated with EC redifferentiation and is also located in *qPRR3.2.* The candidate gene *WOX2a*, which was screened by this SNP, has been confirmed to promote callus regeneration and improve the transformation efficiency of recalcitrant inbred lines [38]. These results indicated that *qPRR3.2* is a "hot spot" region in maize somatic regeneration studies. *qEIR3.1* and *qPRR3.1* are two QTLs with partially overlapping regions on chromosome 3 (Figure 5 and Table 3). The amount of phenotypic variation explained by *qPRR3.1* was the highest among all the loci detected, reaching 14.06% (Table 3). Wang et al. [39] found that sixteen auxin signal transduction pathway genes were differentially expressed in the EC formation period of inbred line 18–599R. The gene *IAA12*, located in the two abovementioned QTLs, was upregulated 25.74-, 39.12- and 29.29-fold in the three stages of callus induction compared with that in the control, indicating that this gene is very sensitive to induction culture. Finally, some candidate genes for EC formation and plantlet regeneration that were obtained in previous studies were also found in other QTLs [8,19,40]. These genes are mainly involved in metabolic pathways, such as signal transduction and redox and stress responses, and may play a key role in maize somatic regeneration.

Su et al. [41] reported that the activity of the *Arabidopsis* stem cell characteristic gene *CLV3* was jointly regulated by WUS and STM proteins. Subsequently, CLV3 and CLE40 bind to receptors, such as CLV1, and complement each other to feedback-regulate the expression of *WUS* and eventually control the homeostasis of shoot stem cells [42]. Within the physical intervals of the QTLs mapped in this study, we screened five *WUS* family genes (*WOX2a*, *WOX5b*, *WOX6*, *WOX11* and *WOX13a*) and four *CLE* family genes (*CLE2*, *CLE6*, *CLE16* and *CLE22*). The function of *WOX2a* in maize somatic regeneration has been verified in previous experiments [43,44], but research on the other genes has not yet been reported. According to the MaizeGDB website, *WOX13a* and *CLE16* are highly expressed in maize shoot apical meristems and developing zygotic embryos, respectively [45]. The qPCR results showed that the expression of *WOX13a* after the initiation of callus induction in H99 was generally higher than that in Fr993, while its expression in the non-regeneration line Fr993 was low and remained stable (Figure 6a). In addition, the expression patterns of *CLE16* in the two parental lines were also quite different (Figure 6b), which preliminarily indicated that *WOX13a* and *CLE16* may be involved in the process of reprogramming the somatic fate of maize cells. Karami et al. [46] found that AHL15 and its homologs are necessary transcription factors for zygotic embryogenesis, and overexpressed *AHL15* can induce *Arabidopsis* seedlings to form somatic embryos under hormone-free conditions. In this study, six *AHL* family genes (*AHL1*, *AHL13*, *AHL22*, *AHL23*, *AHL25* and *AHL27*) were mined in the QTLs. These genes specifically bind to AT-rich DNA sequences that are related to nuclear matrix attachment regions (MARs) and may function in developmental regulation and signal transduction. The expression analysis results revealed that the expression level of *AHL23* was higher in H99 than in Fr993 (Figure 6c), which was consistent with the

previous finding that *AHL* family genes positively regulate somatic embryogenesis [46], suggesting that the *AHL23* gene may also function similarly in maize.

Hormone signal transduction has been shown to be an important pathway in determining plant stem cell fate [47]. Ma et al. [48] found that *Arabidopsis* stem cells were insensitive to auxin because WUS significantly downregulated the expression of *Monopteros/ARF5*, limiting cell differentiation in the central region by reducing auxin signaling. In addition, *Monopteros/ARF5* can also feedback-regulate the activities of *WUS* and *CLV* by repressing *Arabidopsis* response regulators (*ARRs*) and Dornroschen/Enhancer of shoot regeneration 1 (*DRN/ESR1*), thereby maintaining stem cell homeostasis [49]. Here, four auxin signal transduction pathway genes (*IAA12*, *IAA30*, *ARF11* and *ARF23*) were screened. The expression of *ARF11* in Fr993 approached zero with a prolonged induction culture time, while its expression in H99 first decreased and then gradually returned to the initial level (Figure 6d), implying that the stability of the auxin signal maintained by this transcription factor may be a necessary condition for EC formation in maize. The above results lay a theoretical foundation for the molecular breeding of maize lines with somatic cells showing high-frequency regeneration.

**Supplementary Materials:** The following supporting information can be downloaded at: https://www.mdpi.com/article/10.3390/agriculture12030393/s1, Figure S1: Phenotypic distributions of three somatic regeneration traits in 2020 and 2021, Table S1: The detailed components of induction medium, Table S2: The detailed components of differentiation medium, Table S3: Real-time PCR primers of the candidate genes, Table S4: Phenotypic data for the segregating populations in 2020 and 2021, Table S5: Summary of the genetic linkage maps for the $F_2$ population.

**Author Contributions:** Conceptualization, L.D. and D.H.; methodology, L.D., Y.Z. and S.H.; software, L.D. and Y.Z.; validation, L.D., Y.Z. and S.H.; formal analysis, L.D., Y.Z. and S.H.; investigation, L.D., Y.Z., S.H. and D.H.; resources, L.D., D.H. and S.H.; data curation, L.D. and Y.Z.; writing—original draft preparation, L.D.; writing—review and editing, L.D., Y.Z., S.H. and D.H.; visualization, L.D.; supervision, L.D. and D.H.; project administration, L.D.; funding acquisition, L.D. All authors have read and agreed to the published version of the manuscript.

**Funding:** This research was funded by the National Natural Science Foundation of China (grant no. 31901067) and the Agricultural Science and Technology Innovation Program of Jilin Province (grant no. C92070501).

**Institutional Review Board Statement:** Not applicable.

**Informed Consent Statement:** Not Applicable.

**Data Availability Statement:** Data are contained within the article or the Supplementary Materials.

**Conflicts of Interest:** The authors declare no conflict of interest.

## References

1. Green, C.E.; Phillips, R.L. Plant Regeneration from Tissue Cultures of Maize. *Crop Sci.* **1975**, *15*, 417–421. [CrossRef]
2. Binott, J.J.; Songa, J.M.; Ininda, J.; Njagi, E.M.; Machuka, J. Plant regeneration from immature embryos of Kenyan maize in-bred lines and their respective single cross hybrids through somatic ebryogenesis. *Afr. J. Biotechnol.* **2008**, *7*, 981–987.
3. Carvalho, C.H.S.; Bohorova, N.; Bordallo, P.N.; Abreu, L.L.; Valicente, F.H.; Bressan, W.; Paiva, E. Type II callus production and plant regeneration in tropical maize genotypes. *Plant Cell Rep.* **1997**, *17*, 73–76. [CrossRef] [PubMed]
4. Ishida, Y.; Hiei, Y.; Komari, T. Agrobacterium-mediated transformation of maize. *Nat. Protoc.* **2007**, *2*, 1614–1621. [CrossRef] [PubMed]
5. Raji, J.A.; Frame, B.; Little, D.; Santoso, T.J.; Wang, K. Agrobacterium- and Biolistic-Mediated Transformation of Maize B104 Inbred. *Maize* **2018**, *1676*, 15–40. [CrossRef]
6. Yadava, P.; Abhishek, A.; Singh, R.; Singh, I.; Kaul, T.; Pattanayak, A.; Agrawal, P.K. Advances in Maize Transformation Technologies and Development of Transgenic Maize. *Front. Plant Sci.* **2017**, *7*, 1949. [CrossRef]
7. Liu, B.; Shan, X.; Wu, Y.; Su, S.; Li, S.; Liu, H.; Han, J.; Yuan, Y. iTRAQ-based quantitative proteomic analysis of embryogenic and non-embryogenic calli derived from a maize (*Zea mays* L.) inbred line Y423. *Int. J. Mol. Sci.* **2018**, *19*, 4004. [CrossRef]
8. López-Ruiz, B.A.; Juárez-González, V.T.; Sandoval-Zapotitla, E.; Dinkova, T.D. Development-Related miRNA Expression and Target Regulation during Staggered In Vitro Plant Regeneration of Tuxpeño VS-535 Maize Cultivar. *Int. J. Mol. Sci.* **2019**, *20*, 2079. [CrossRef]

9. Shen, Y.; Jiang, Z.; Yao, X.; Zhang, Z.; Lin, H.; Zhao, M.; Liu, H.; Peng, H.; Li, S.; Pan, G. Genome Expression Profile Analysis of the Immature Maize Embryo during Dedifferentiation. *PLoS ONE* **2012**, *7*, e32237. [CrossRef]
10. Abhishek, A.; Karjagi, C.G.; Nath, R.; Bhardwaj, M.; Ramteke, P.W.; Kumar, P.; Dass, S.; Kumar, R.S. Differential effect of immature em-bryo's age and genotypes on embryogenic type II callus production and whole plant regeneration in tropical maize inbred lines (*Zea mays* L.). *Indian J. Genet. Plant Breed* **2014**, *74*, 317–324. [CrossRef]
11. Rakshit, S.; Rashid, Z.; Sekhar, J.C.; Fatma, T.; Dass, S. Callus induction and whole plant regeneration in elite Indian maize (*Zea mays* L.) inbreds. *Plant Cell Tissue Organ Cult.* **2010**, *100*, 31–37. [CrossRef]
12. Ikeuchi, M.; Favero, D.S.; Sakamoto, Y.; Iwase, A.; Coleman, D.; Rymen, B.; Sugimoto, K. Molecular mechanisms of plant regeneration. *Annu. Rev. Plant. Biol.* **2019**, *70*, 377–406. [CrossRef] [PubMed]
13. Song, Y.; Xia, Y.-L.; Wei, X.; Zhang, Z.-M.; Zhao, M.-J.; Rong, T.-Z.; Pang, G.-T. Analysis of Gene Effect on Four Characters of Immature Embryo Culture in Maize. *Agric. Sci. China* **2007**, *6*, 1291–1296. [CrossRef]
14. Krakowsky, M.D.; Lee, M.; Garay, L.; Woodman-Clikeman, W.; Long, M.J.; Sharopova, N.; Frame, B.; Wang, K. Quantitative trait loci for callus initiation and totipotency in maize (*Zea mays* L.). *Theor. Appl. Genet.* **2006**, *113*, 821–830. [CrossRef]
15. Pan, G.; Zhang, Z.; Wei, X.; Song, Y.; Zhao, M.; Xia, Y. QTL Analysis of maize (*Zea mays* L.) embryo culturing capacity. *Acta Agron. Sin.* **2006**, *32*, 7–13.
16. Zhang, X.-L.; Long, Y.; Ge, F.; Guan, Z.-R.; Zhang, X.-X.; Wang, Y.-L.; Shen, Y.; Pan, G.-T. A genetic study of the regeneration capacity of embryonic callus from the maize immature embryo culture. *Hereditas* **2017**, *39*, 143–155.
17. Armstrong, C.L.; Romero-Severson, J.; Hodges, T.K. Improved tissue culture response of an elite maize inbred through back-cross breeding, and identification of chromosomal regions important for regeneration by RFLP analysis. *Theor. Appl. Genet.* **1992**, *84*, 755–762. [CrossRef]
18. Lowe, B.A.; Way, M.M.; Kumpf, J.M.; Rout, J.; Warner, D.; Johnson, R.; Armstrong, C.L.; Spencer, M.T.; Chomet, P.S. Marker assisted breeding for transformability in maize. *Mol. Breed.* **2006**, *18*, 229–239. [CrossRef]
19. Ma, L.; Liu, M.; Yan, Y.; Qing, C.; Zhang, X.; Zhang, Y.; Long, Y.; Wang, L.; Pan, L.; Zou, C.; et al. Genetic dissection of maize embryonic callus regenerative capacity using multi-locus genome-wide association studies. *Front. Plant Sci.* **2018**, *9*, 561. [CrossRef]
20. Zhang, X.; Wang, Y.; Yan, Y.; Peng, H.; Long, Y.; Zhang, Y.; Jiang, Z.; Liu, P.; Zou, C.; Peng, H.; et al. Transcriptome sequencing analysis of maize embryonic callus during early redifferentiation. *BMC Genom.* **2019**, *20*, 1–22. [CrossRef]
21. Ge, F.; Qu, J.; Liu, P.; Pan, L.; Zou, C.; Yuan, G.; Yang, C.; Pan, G.; Huang, J.; Ma, L.; et al. Genome assembly of the maize inbred line A188 provides a new reference genome for functional genomics. *Crop J.* **2021**, *10*, 47–55. [CrossRef]
22. Henderson, C.B. *Maize Research and Breeders Manual*, 8th ed.; Illinois Foundation Seeds Inc.: Champaign, IL, USA, 1976.
23. Knapp, S.J.; Stroup, W.W.; Ross, W.M. Exact Confidence Intervals for Heritability on a Progeny Mean Basis. *Crop Sci.* **1985**, *25*, 192–194. [CrossRef]
24. Guo, Z.; Wang, H.; Tao, J.; Ren, Y.; Xu, C.; Wu, K.; Zou, C.; Zhang, J.; Xu, Y. Development of multiple SNP marker panels affordable to breeders through genotyping by target sequencing (GBTS) in maize. *Mol. Breed.* **2019**, *39*, 37. [CrossRef]
25. Van Ooijen, J.W. *Joinmap 4.0, Software for the Calculation of Genetic Linkage Maps in Experimental Populations*; Kyazma BV: Wageningen, The Netherlands, 2006.
26. Lincoln, S.; Daly, M.; Lander, E. *Mapping Genetic Mapping with MAPMAKER/EXP3.0*; Whitehead Institute Technical Report: Cambridge, MA, USA, 1992.
27. Kosambi, D.D. The estimation of map distances from recombination values. *Ann. Eugen.* **1943**, *12*, 172–175. [CrossRef]
28. Zeng, Z.B. Precision mapping of quantitative trait loci. *Genetics* **1994**, *136*, 1457–1468. [CrossRef]
29. Wang, S.; Basten, C.; Zeng, Z. *Windows QTL Cartographer 2.5*; Department of Statistics, North Carolina State University: Raleigh, NC, USA, 2012.
30. Schefe, J.H.; Lehmann, K.E.; Buschmann, I.R.; Unger, T.; Funke-Kaiser, H. Quantitative real-time RT-PCR data analysis: Cur-rent concepts and the novel "gene expression's CT difference" formula. *J. Mol. Med.* **2006**, *84*, 901–910. [CrossRef]
31. Alejandri-Ramírez, N.D.; Chávez-Hernández, E.C.; Contreras-Guerra, J.L.; Reyes, J.L.; Dinkova, T.D. Small RNA differential expression and regulation in Tuxpeño maize embryogenic callus induction and establishment. *Plant Physiol. Biochem.* **2018**, *122*, 78–89. [CrossRef]
32. Li, H.; Zhang, J.; Yang, Y.; Jia, N.; Wang, C.; Sun, H. miR171 and its target gene SCL6 contribute to embryogenic callus in-duction and torpedo-shaped embryo formation during somatic embryogenesis in two lily species. *Plant Cell Tiss. Org.* **2017**, *130*, 591–600. [CrossRef]
33. Suo, J.; Zhou, C.; Zeng, Z.; Li, X.; Bian, H.; Wang, J.; Zhu, M.; Han, N. Identification of regulatory factors promoting embryogenic callus formation in barley through transcriptome analysis. *BMC Plant Biol.* **2021**, *21*, 1–19. [CrossRef]
34. Wójcikowska, B.; Botor, M.; Morończyk, J.; Wójcik, A.M.; Nodzyński, T.; Karcz, J.; Gaj, M.D. Trichostatin A triggers an embryo-genic transition in Arabidopsis explants via an auxin-related pathway. *Front. Plant. Sci.* **2018**, *9*, 1353. [CrossRef]
35. Ali, F.; Ahsan, M.; Saeed, N.A.; Ahmed, M.; Ali, Q.; Kanwal, N.; Tehseen, M.M.; Ijaz, U.; Bibi, I.; Niazi, N.K. Establishment and optimization of callus-to-plant re-generation system using mature and immature embryos of maize (*Zea mays*). *Int. J. Agric. Biol.* **2014**, *16*, 111–117.
36. Zhang, H.; Liu, Y.; Guo, X.; Zhang, F.; Li, J.; Chen, G.; Dongfa, S. QTL mapping for callus induction and plant regeneration in maize immature embryos. *Acta Agron. Sin.* **2006**, *32*, 385–389.

37. Salvo, S.; Cook, J.; Carlson, A.R.; Hirsch, C.N.; Kaeppler, S.M.; Kaeppler, H.F. Genetic Fine-Mapping of a Quantitative Trait Locus (QTL) Associated with Embryogenic Tissue Culture Response and Plant Regeneration Ability in Maize (*Zea mays* L.). *Plant Genome* **2018**, *11*, 170111. [CrossRef] [PubMed]
38. Lowe, K.; Wu, E.; Wang, N.; Hoerster, G.; Hastings, C.; Cho, M.-J.; Scelonge, C.; Lenderts, B.; Chamberlin, M.; Cushatt, J.; et al. Morphogenic Regulators Baby boom and Wuschel Improve Monocot Transformation. *Plant Cell* **2016**, *28*, 1998–2015. [CrossRef]
39. Wang, Y.; He, S.; Long, Y.; Zhang, X.; Zhang, X.; Hu, H.; Li, Z.; Hou, F.; Ge, F.; Gao, S.; et al. Genetic variations in ZmSAUR15 contribute to the formation of immature embryo-derived embryonic calluses in maize. *Plant J.* **2021**, *109*, 980–991. [CrossRef]
40. Ge, F.; Luo, X.; Huang, X.; Zhang, Y.; He, X.; Liu, M.; Lin, H.; Peng, H.; Li, L.; Zhang, Z.; et al. Genome-wide analysis of transcription factors involved in maize embryonic callus formation. *Physiol. Plant.* **2016**, *158*, 452–462. [CrossRef]
41. Su, Y.; Zhou, C.; Li, Y.; Yu, Y.; Tang, L.; Zhang, W.; Yao, W.J.; Huang, R.; Laux, T.; Zhang, X.S. Integration of pluripotency pathways regulates stem cell maintenance in the Arabidopsis shoot meristem. *Proc. Natl. Acad. Sci. USA* **2020**, *117*, 202015248. [CrossRef]
42. Schlegel, J.; Denay, G.; Wink, R.; Pinto, K.G.; Stahl, Y.; Schmid, J.; Blümke, P.; Simon, R.G. Control of Arabidopsis shoot stem cell homeostasis by two antagonistic CLE peptide signalling pathways. *eLife* **2021**, *10*, 70934. [CrossRef]
43. Lowe, K.; La Rota, M.; Hoerster, G.; Hastings, C.; Wang, N.; Chamberlin, M.; Wu, E.; Jones, T.; Gordon-Kamm, W. Rapid genotype "independent" *Zea mays* L. (maize) transformation via direct somatic embryogenesis. *In Vitro Cell. Dev. Biol.-Plant* **2018**, *54*, 240–252. [CrossRef]
44. Mookkan, M.; Nelson-Vasilchik, K.; Hague, J.; Zhang, Z.; Kausch, A.P. Selectable marker independent transformation of recalcitrant maize inbred B73 and sorghum P898012 mediated by morphogenic regulators BABY BOOM and WUSCHEL2. *Plant Cell Rep.* **2017**, *36*, 1477–1491. [CrossRef]
45. Walley, J.W.; Sartor, R.C.; Shen, Z.X.; Schmitz, R.J.; Wu, K.J.; Urich, M.A.; Nery, J.R.; Smith, L.G.; Schnable, J.C.; Ecker, J.R.; et al. Integration of omic networks in a developmental atlas of maize. *Science* **2016**, *353*, 814–818. [CrossRef] [PubMed]
46. Karami, O.; Rahimi, A.; Mak, P.; Horstman, A.; Boutilier, K.; Compier, M.; van der Zaal, B.; Offringa, R. An Arabidopsis AT-hook motif nuclear protein mediates somatic embryogenesis and coinciding genome duplication. *Nat. Commun.* **2021**, *12*, 2058. [CrossRef] [PubMed]
47. Lopes, F.L.; Galvan-Ampudia, C.; Landrein, B. WUSCHEL in the shoot apical meristem: Old player, new tricks. *J. Exp. Bot.* **2021**, *72*, 1527–1535. [CrossRef] [PubMed]
48. Ma, Y.; Miotk, A.; Šutiković, Z.; Ermakova, O.; Wenzl, C.; Medzihradszky, A.; Gaillochet, C.; Forner, J.; Utan, G.; Brackmann, K.; et al. WUSCHEL acts as an auxin response rheostat to maintain apical stem cells in Arabidopsis. *Nat. Commun.* **2019**, *10*, 1–11. [CrossRef]
49. Luo, L.; Zeng, J.; Wu, H.; Tian, Z.; Zhao, Z. A Molecular Framework for Auxin-Controlled Homeostasis of Shoot Stem Cells in Arabidopsis. *Mol. Plant* **2018**, *11*, 899–913. [CrossRef]